AJNR

Neurointerventions in Children: Radiation Exposure and Its Import

D.B. Orbach, C. Stamoulis, K.J. Strauss, J. Manchester, E.R. Smith, R.M. Scott and N. Lin

AJNR Am J Neuroradiol published online 24 October 2013
http://www.ajnr.org/content/early/2013/10/24/ajnr.A3758

Published October 24, 2013 as 10.3174/ajnr.A3758

Neurointerventions in Children: Radiation Exposure and Its Import

D.B. Orbach, C. Stamoulis, K.J. Strauss, J. Manchester, E.R. Smith, R.M. Scott, and N. Lin

ABSTRACT

BACKGROUND AND PURPOSE: Neurointerventions in children have dramatically improved the clinical outlook for patients with previously intractable cerebrovascular conditions, such as vein of Galen malformations and complex arteriovenous fistulas. However, these complex and sometimes lengthy procedures are performed under fluoroscopic guidance and thus unavoidably expose vulnerable pediatric patients to the effects of ionizing radiation. Recent epidemiologic evidence from a national registry of children who underwent CT scans suggests a higher-than-expected incidence of secondary tumors. We sought to calculate the predicted risk of secondary tumors in a large cohort of pediatric neurointerventional patients.

MATERIALS AND METHODS: We reviewed our cohort of pediatric neurointerventions, tabulated radiation dose delivered to the skin, and calculated the range of likely brain-absorbed doses by use of previously developed mathematical models. The predicted risk of secondary tumor development as a function of brain-absorbed dose in this cohort was then generated by use of the head CT registry findings.

RESULTS: Maximal skin dose and brain-absorbed doses in our cohort were substantially lower than have been previously described. However, we found 1) a statistically significant correlation between radiation dose and age at procedure, as well as number and type of procedures, and 2) a substantial increase in lifetime predicted risk of tumor above baseline in the cohort of young children who undergo neurointerventions.

CONCLUSIONS: Although neurointerventional procedures have dramatically improved the prognosis of children facing serious cerebrovascular conditions, the predicted risk of secondary tumors, particularly in the youngest patients and those undergoing multiple procedures, is sobering.

ABBREVIATIONS: MSD = maximal skin dose; RAD-IR = Radiation Doses in Interventional Radiology Procedures

Children undergoing fluoroscopy are exposed to ionizing radiation. Commonly used measures of tumor risk from this exposure are based on decades of observations in survivors from the regions surrounding Hiroshima and Nagasaki, as summarized in BEIR-VII.[1] However, a recent study[2] analyzing a national registry in the United Kingdom of >178,000 children who underwent CT scans reported a higher incidence of brain tumors and leukemia than would be expected on the basis of the BEIR data. For children undergoing neurointerventions, these results suggest that previous predictions may underestimate the actual rate of radiation-related tumor development.

We retrospectively analyzed our data base of radiation doses delivered to a cohort of children who underwent 355 cerebral angiograms and neurointerventions at a single high-volume pediatric cerebrovascular center. We converted the reported maximal skin dose (MSD) to an estimate of the range of brain-absorbed doses by use of previously derived age-based conversion factors.[3,4] On the basis of recent data from the UK CT study, we then estimated the predicted risk of brain tumors in this cohort, related to the procedures that the children underwent.

MATERIALS AND METHODS

Approval was obtained from the Institutional Review Board at Boston Children's Hospital for retrospective review of our neuro-

Received July 16, 2013; accepted after revision August 11.

From the Division of Neurointerventional and Interventional Radiology (D.B.O., J.M.), Departments of Radiology (C.S., J.M.), Neurology (C.S.), and Neurosurgery (E.R.S., R.M.S.), Children's Hospital Boston, Boston, Massachusetts; Harvard Medical School (D.B.O., C.S., E.R.S., R.M.S.), Boston, Massachusetts; Department of Radiology (K.J.S.), Cincinnati Children's Hospital Medical Center, Cincinnati, Ohio; and Departments of Radiology and Neurosurgery (N.L.), Brigham and Women's Hospital, Boston, Massachusetts.

Please address correspondence to Darren B. Orbach, MD, PhD, Neurointerventional Radiology, Children's Hospital Boston, 300 Longwood Ave, Boston, MA 02115; e-mail: darren.orbach@childrens.harvard.edu

http://dx.doi.org/10.3174/ajnr.A3758

Table 1: Distribution of number of procedures per patient and number of procedures per age bracket

No. of Procedures per Patient	No. of Patients	Age Cohort	No. of Cases
1	125	<1 year	27
2	42	1–2 years	37
3	20	3–7 years	80
4	5	8–13 years	101
5	4	13–17 years	91
6	2	18–20 years	19
7	2		
9	1		
11	1		

Note:—Total number of procedures = 355; total number of unique patients = 202. Most patients underwent a single procedure, the vast majority underwent 3 or fewer, and a very small number underwent 5 or more. The mean age of the cohort was 9.7 years.

interventional data base of children younger than 21 years of age who underwent cerebral angiography and/or transarterial neuroembolization between September 2006 and June 2012; percutaneous procedures, such as sclerotherapy, were not included. The included procedures were performed by a single operator (D.B.O.) on 1 of 2 Axiom Artis biplane flat-panel fluoroscopic units (Siemens, Erlangen, Germany).

The radiation physicist at Boston Children's Hospital worked with a Siemens design engineer in 2005 to create examination-set protocols tailored to patient size (age) and body part, with fluoroscopy and DSA. This resulted in skin dose rate reductions up to 30% relative to standard configurations, depending on the type of examination and thickness of the patient. A dose data base was installed: Patient Exposure Management Network (PEMNET, Clinical Microsystems, Arlington, Virginia). PEMNET automatically captures the uncalibrated cumulative air kerma data at the end of each procedure and additionally captures C-arm angles of multiple projections used during a procedure, needed to estimate peak skin dose from cumulative air kerma. Before the implementation of PEMNET, radiation data were not consistently stored. During the time range, radiation dose information was available for 355 cases. Skin radiation dose can be calculated as follows:

Skin dose $\sim AK \times CF \times ISL \times BS$, where

AK = displayed cumulative air kerma; CF = calibration factor for displayed air kerma ~1; ISL = inverse square law correction for entrance skin plane versus interventional reference point at which air kerma meter is calibrated, ~0.8; and BS = backscatter factor, ~1.4–1.45 for skull, depending on patient age.[5]

CF is 1 ± 5%, with appropriate annual measurement and adjustment by a medical physicist. Because the entrance plane of the patient's head positioned at isocenter is 5–9 cm from the interventional reference point, depending on patient size, ISL ranges from 0.75–0.85.

We tabulated the number of procedures undergone by each patient and the distribution of procedures by patient age (Table 1). The descriptive statistics for maximal skin radiation dose (in each plane and in total) and fluoroscopy time as a function of procedure type and as a function of the date of the study are summarized in Table 2. MSD values in the frontal and lateral imaging planes were corrected for age by multiplying by the following scaling factors: for age ≤5 years, 1.12 for frontal plane, 1.06 for lateral plane, and for age >5 years, 1.24 for frontal plane, 1.16 for lateral plane. There were 175 cases between September 2006 and June 2010 and 180 cases between July 2010 and June 2012 (Table 2). Mean MSD and fluoroscopy time stratified by patient age are summarized in Table 3. Cumulative MSD statistics, stratified by number of procedures, are summarized in Table 4.

Using the conversion factors generated by mathematical modeling and the Radiation Doses in Interventional Radiology Procedures (RAD-IR) study data (in particular, Table 6 of Thierry-Chef et al.),[3,4] we converted the maximal skin dose to estimates of absorbed brain dose. Absorbed brain dose varies widely (by a factor of 4–8), depending on whether tight collimation and varying positions for the imaging system were used. Following the lead of the RAD-IR investigators, we accordingly report the brain-absorbed doses under the 2 conditions of tight and wide collimation separately (Tables 4 and 5).

We extrapolated the increased risk of brain tumors above the expected baseline, hereafter referred to as predicted risk, attributable to the absorbed brain dose in our cohort, by use of a linear no-threshold model and the values for excess relative risk per mGy exposure reported by the UK CT study investigators.[2]

Statistical Analysis

All analyses were performed at the patient level.

Regression. To assess the correlation between type of procedure(s) and cumulative radiation dose and the effect of patient age on that correlation, we developed an ordinary regression model with (cumulative) radiation dose as the outcome and procedure type, age, and number of procedures as the explanatory (independent) variables. For patients with multiple procedures, age at the last procedure was included. Procedure type was modeled as a categoric variable. For patients with 1 procedure, type = 1 for angiogram and type = 2 otherwise (implying embolization). For patients with multiple procedures, type = 1 if all procedures were angiograms and type = 2 otherwise. All statistical analysis was performed with the use of Matlab (MathWorks, Natick, Massachusetts) and R (www.r-project.org).

Estimation of Predicted Risk. In the absence of a clinical outcome (cancer) for this cohort, we estimated predicted risk for tumors based on the data in the UK study.[2] In that study, a linear relationship between relative risk and absorbed brain dose radiation was estimated, with slope of the fitted line 0.023 and intercept 1. Note that in our study, predicted risk was estimated on the basis of cumulative radiation doses, that is, at the patient level rather than at the case level. For patients who underwent only 1 procedure, case and patient radiation levels are identical. However, for patients who underwent multiple procedures, we were interested in cancer risk after cumulative exposure.

RESULTS

The 355 procedures in our data base with available radiation data were performed in 202 unique patients. Whereas the mean number of procedures per patient was 1.8, the underlying distribution was skewed, with most patients undergoing 1 procedure, 83% undergoing 2 or fewer procedures, and <3% undergoing 6 or more procedures. The age range of our cohort was 4 days to 20

Table 2: Maximal skin dose of radiation (in mGy) and fluoroscopy time per procedure (in minutes), as a function of case type and date

Case Type	Dates	Mean Radiation Dose, Frontal Plane, mGy	SD Radiation Dose Frontal Plane, mGy	Mean Radiation Dose, Lateral Plane, mGy	SD Radiation Dose, Lateral Plane, mGy	Mean Radiation Dose, Total, mGy	SD Radiation Dose, Total, mGy	Fluoroscopy Time, Frontal Plane, min	Fluoroscopy Time, Lateral Plane, min
All cases	9/06–6/10	319	289.6	201.2	279.2	520.2	498.9	26.7	22.2
	7/10–6/12	215.6	211.5	112.4	186.9	328	350.1	17.9	12.6
Diagnostic angiograms	All	164.9	161.1	74.6	69.5	239.4	217.5	11.2	6.2
	9/06–6/10	185.7	212.7	88	86.8	273.7	284.9	10.9	6.4
	7/10–6/12	150	109.1	65	52.2	215	148.6	11.4	6.1
Embolizations	All	449.4	306	298.4	345	747.7	540.6	42.4	37.4
	9/06–6/10	482.2	290.7	340.5	364.9	822.7	542.6	48.8	44.5
	7/10–6/12	430.5	303.1	267.2	343.9	697.7	531.8	34.5	28.8

Note:—SD indicates standard deviation (inter-case variability).

Table 3: Maximal skin dose of radiation and the fluoroscopy time per procedure as stratified by patient age

Age, y	Radiation Dose, Frontal Plane, mGy	SD Radiation Dose, Frontal Plane, mGy	Radiation Dose, Lateral Plane, mGy	SD Radiation Dose, Lateral Plane, mGy	Radiation Dose, Total, mGy	SD Radiation Dose, Total, mGy	Fluoroscopy Time, Frontal Plane, min	Fluoroscopy Time, Lateral Plane, min
<1	186.7	168.3	186.2	198.5	372.9	361.2	40.5	37.7
1–2	296.3	350.3	147.2	109.3	443.5	434.4	26.1	22.5
3–7	236	241.3	147.2	189.3	383.3	398.9	24.0	17.6
8–12	244.5	233.4	110.8	131	355.3	341.9	19.1	14.6
13–17	329.	292	192.2	318.7	521.3	529.7	17.8	13.1
18–21	328.5	260.2	255.1	553.6	583.5	729.3	19.5	12.6
All ages	266.6	257.9	156.2	240.7	422.7	440	21.9	17.0

Note:—SD indicates standard deviation (inter-procedure variability).

Table 4: Maximal cumulative skin radiation dose stratified by number of procedures

No. of Procedures	No. of Patients	Mean Age, y	SD Age, y	Mean Radiation Dose, Total, mGy	SD Radiation Dose, Total, mGy	Mean Radiation Dose, Embolizations, mGy	SD Radiation Dose, Embolizations, mGy	Mean Radiation Dose, Angiograms, mGy	SD Radiation Dose, Angiograms, mGy
1	125	10.2	5.97	318.2	409.9	643.4	730.8	232.8	202.4
2	42	10.1	5.5	1330.2	784.8	598.7	538.9	514.6	318.8
3	20	9.5	5.7	1131.5	862.1	2677.8	1017.9	535.6	269
4	5	8.3	4.9	1207.4	392.9	1736.1	–	–	–
5	4	11.4	5.8	2204.8	791.4	1814.1	–	–	–
6	2	10.3	12.1	582.3	168.3	–	–	–	–
7	2	5.1	1.5	4749.0	1737.6	–	–	–	–
9	1	6.3	–	8625.7	–	–	–	–	–
11	1	15.05	–	5563.3	–	–	–	–	–

Note:—For patients with multiple procedures, the age at the last procedure is reported, and embolizations or angiogram doses are reported only for those patients with all procedures of the same type.
SD indicates standard deviation (inter-patient variability).

years, with a mean age of 9.7 years, and standard deviation (SD) of 5.8 years. The distribution of cases among patients and the breakdown of number of cases for each age cohort are presented in Table 1. Although some pathologies such as brain AVM, pial fistulas, aneurysms, dural fistulas, and extracranial AVM or AVF were found in all age groups, particular conditions occurred exclusively in subsets of the cohort, such as vein of Galen malformation in the <1-year and 1- to 2-year age groups.

At the doses received by our cohort, deterministic effects of radiation were nearly entirely absent, with a single case of transient hair loss (possibly related to scalp positioning) and a single case of transient scalp erythema.

As expected, the radiation dose associated with diagnostic cerebral angiography was significantly lower than that associated with embolizations, with the mean dose of the former <50% the mean dose of the latter (Table 2). When we split the cohort by date of procedure, with approximately equivalent numbers of procedures from September 2006 to June 2010 and from July 2010 to June 2012, there was a statistically significant decrease in mean total dose across all cases in the later cohort as compared with the earlier ($P < .0001$). When angiography and embolization procedures were examined separately, there was a statistically significant decrease in mean total dose for angiograms after July 2010 ($P = .04$) but a statistically nonsignificant decrease in dose for embolizations ($P = .09$). A nonparametric Wilcoxon rank sum test was used to test statistical significance.

On the basis of the regression analysis, procedure type and number of procedures were statistically significant predictors of radiation dose, and the effect of age at procedure was also statistically significant. The results of this analysis and model parameters are summarized in Table 7. The model was overall statistically significant ($P < .0001$), with a coefficient of determination $R^2 = 0.67$, which suggests an adequate fit to the data.

Because of the differences in conversion factors for MSD to

Table 5: Large (uncollimated), uniform field condition: brain absorbed dose of radiation and relative risk of developing brain tumors as a function of patient age

Age, y	MSD, Both Planes, mGy	SD, Both Planes, mGy	Brain Dose–to–MSD Conversion Factor	Brain-Absorbed Dose, mGy	Projected Risk of Developing Brain Tumors (×Baseline)
<1	372.9	361.2	0.48	164.4	4.8
1–2	443.5	434.4	0.38	160.0	4.7
3–7	383.3	398.9	0.30	93.3	3.2
8–12	355.3	341.9	0.25	74.1	2.7
13–17	521.3	529.7	0.24	103.9	3.4
18–21	583.5	729.3	0.23	106.3	3.4
All ages	422.7	440	0.25	90.1	3.1

Note:—Projected risk is calculated as (excess relative risk = 0.023/mGy)+1.
SD indicates standard deviation (inter-patient variability).

Table 6: Small (collimated), non-uniform field condition: brain-absorbed dose of radiation and excess relative risk of developing brain tumors as a function of patient age

Age, y	MSD, Both Planes, mGy	SD, Both Planes, mGy	Brain Dose–to–MSD Conversion Factor	Brain-Absorbed Dose, mGy	Projected Risk of Developing Brain Tumors (×Baseline)
<1	372.9	361.2	0.14	47.9	2.1
1–2	443.5	434.4	0.11	46.3	2.1
3–7	383.3	398.9	0.09	28.0	1.6
8–12	355.3	341.9	0.05	14.8	1.3
13–17	521.3	529.7	0.03	13.0	1.3
18–21	583.5	729.3	0.03	13.9	1.3
All ages	422.7	440	0.08	18.0	1.4

Note:—Projected risk is calculated as (excess relative risk = 0.023/mGy)+1.
SD indicates standard deviation (inter-patient variability).

Table 7: Linear regression model parameters including regression coefficients, their confidence intervals, *P* values, and Wald statistic values

Parameter	Coefficient (*b*)	Confidence Interval	Standard Error	*P* Value	Wald Statistic
Intercept	−1081.1	[−1403.4, −0.7587]	163.5	<.0001	43.7
Age at procedure	18.6	[3.1, 34.0]	7.8	.018	5.6
Procedure type	454.9	[261.7, 648.2]	98.0	<.0001	21.5
No procedures	555.5	[487.7, 623.3]	34.4	<.0001	260.9

brain-absorbed dose as a function of age, the brain-absorbed dose showed greater differences across age groups (varying by a factor of >2.2) than did the MSD (Table 5). The highest mean brain-absorbed dose was in the <1-year-old subgroup, followed by the 1- to 2-year-old subgroup. In the case of tight collimation (Table 5), brain-absorbed doses dropped markedly in every age group, but the differences across age groups increased further (varying by a factor of 3.7).

Estimated predicted risk, as a function of age at last exposure, is shown in Fig 1 (for small and large radiation field conditions; top and bottom, respectively), along with the fitted regression line. There was no clear correlation between projected relative risk and age at last exposure for large uniform field conditions. There was a statistically significant relationship between age at last exposure and projected relative risk under small nonuniform field conditions (on the basis of a linear regression model for risk as a function of age, $b = -0.08$, $P = .001$, Wald statistic = 10.8). There was no statistically significant relationship between projected relative risk and age under large uniform field conditions ($b = -0.087$, $P = .33$). The distribution of predicted risk for our cohort is shown in the histogram in Fig 2. Although for most patients (~80%) predicted risk was in the range of 1–2 times baseline for small field conditions and 1–5 times baseline for large field conditions, for ~20% of patients, predicted risk was substantially higher: 3–15 times baseline for small field conditions and 9–57 times baseline for large field conditions.

Finally, we also examined predicted risk as a function of age, separately, only for the subset of patients with 1 procedure, under both field conditions (Fig 3). There was a statistically significant relationship between age at exposure and predicted risk for small nonuniform field conditions ($b = 0.012$, $P = .004$, Wald statistic = 8.58). There was no statistically significant relationship between age at exposure and projected risk for large uniform field conditions ($b = 0.018$, $P = .11$).

DISCUSSION

Several recent studies have documented the overall procedural safety of cerebral angiography in children at high-volume centers.[6,7] However, both diagnostic cerebral angiography and transcatheter cerebral interventions are performed under fluoroscopic visualization, and as such, unavoidably expose patients to ionizing radiation. Children are more vulnerable to deleterious effects from radiation than are adults, with increasing vulnerability at younger ages. Neurointerventions, with their inherent risk, are complex and lengthy and are associated with prolonged periods of fluoroscopic exposure to patients. Thus, outside of patients undergoing radiation therapy procedures, children who undergo neurointerventions are potentially at greatest risk of having iatrogenic adverse effects from ionizing radiation.

Although we focus here on the stochastic effects of incident radiation, we did find an extremely low incidence of deterministic adverse events relatable to radiation, with only 2 deterministic adverse events, both transient, in the total cohort.

The most detailed and careful prior study of pediatric radiation doses from neurointerventions (in 49 children) was performed[3,4] as a subset of the larger RAD-IR study.[8-10] The investigators described the maximal skin dose delivered, calculated probable absorbed brain doses, and predicted the expected increase in incidence of brain tumors as a result of this exposure. The MSD and brain-absorbed doses that we report here are substantially lower than those reported for the 49 children who underwent neurointerventions in RAD-IR, probably a reflection both of technological improvements in the time since that earlier study, and of our fluoroscopy parameters, highly optimized for procedures in children.[3,4]

After splitting the cohort into 2 approximately equal subsets by date of procedure, we found that the radiation dose in the more recent subset was markedly lower for the set of procedures performed in the last 2 years. There was a statistically significant

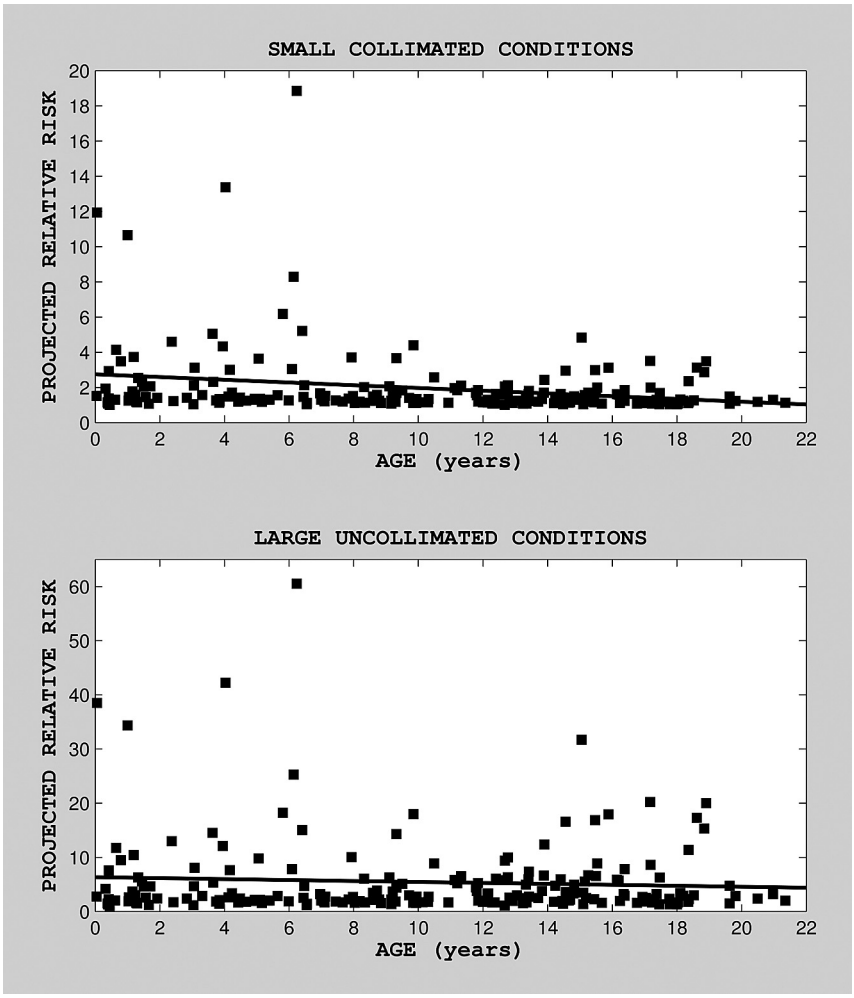

FIG 1. Projected relative risk as a function of age at (last) exposure, under nonuniform (top) and uniform (bottom) field conditions. Median predicted (projected) risk was 1.34 (mean = 1.96, SD = 2; range, 1.0–18.85) under small nonuniform field conditions and 2.72 (mean = 5.45, SD = 7.36; range, 1.02–60.5) under large uniform field conditions.

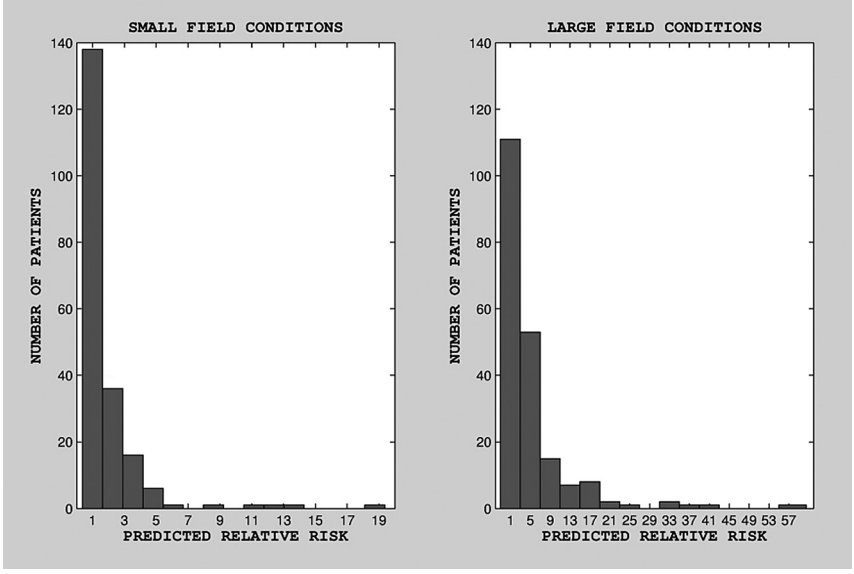

FIG 2. Distribution of projected relative risk under small (left) and large (right) field conditions.

decrease in total radiation dose for these procedures, as well as specifically for angiograms in the last 2 years, but no statistically significant decrease in embolization doses. Because there were no changes in hardware or software during this time range that could explain this diminution in radiation dose, this change over time may relate to progressively increased attention paid to radiation dose by the primary operator (D.B.O.), with ongoing time at a dedicated pediatric facility. Most embolization procedures are already tightly focused, with angiography performed in the target vessels before and after the embolization and with relatively little flexibility for performing fewer angiographic runs. Diagnostic angiography, on the other hand, allows the pediatric practitioner significant latitude in terms of limiting what vessels are injected, how many views are obtained, and so forth.

Comparing the <1-year cohort with the 13- to 17-year cohort in Table 3 shows that whereas fluoroscopy time was markedly higher in infants, MSD was much lower; this effect is largely caused by the small body size of the youngest patients. Additionally, fewer DSA runs tend to be performed in the infants, as road-mapping and other image-store techniques are maximally utilized.

It is likely that some of the differences in MSD with stratification by age (Table 3) result from particularities of the pathology seen at various ages. For example, the 3- to 7-year and 8- to 12-year cohorts, which had the lowest MSD, are notable for a preponderance of Moyamoya cases, in nearly all of which the procedure performed was diagnostic angiography, either before surgery or at 1-year postsynangiosis follow-up, rather than embolizations.

In shifting the focus from MSD to brain-absorbed dose (Tables 4 and 5), the highest doses were seen in the youngest patients (<1 year), followed by the next-youngest cohort (1–2 years). Thus biologic factors, such as low skull thickness and attenuation in the youngest patients, resulting in brain absorption of a very high fraction of the radiation incident on the skin, are the key operative determinants of radiation dose delivered to the brain.

The degree of increase in lifetime relative risk of development of brain tumor

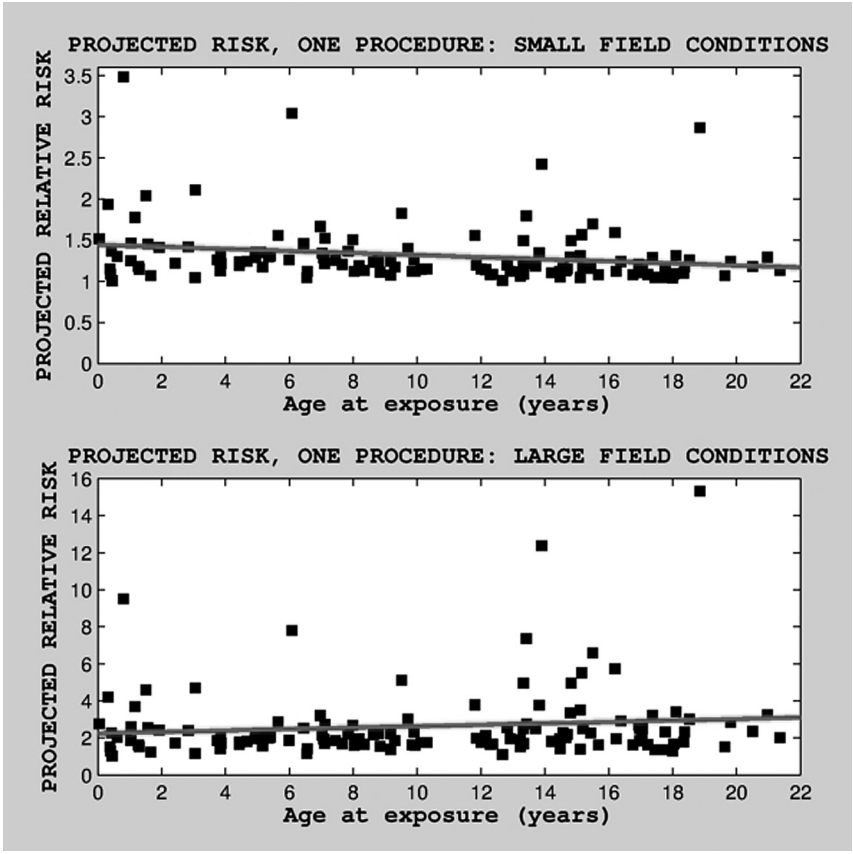

FIG 3. Projected relative risk as a function of age at (last) exposure, under nonuniform (top) and uniform (bottom) field conditions, for subjects with only 1 procedure and thus no cumulative radiation exposure caused by multiple procedures. Median projected risk was 1.2 (mean = 1.31, SD = 0.37; range, 1.0–3.48) for small nonuniform field condition and 2.03 (mean = 2.6, SD = 2; range, 1.02–15.32) for large uniform field conditions.

reported here is higher than has been previously reported. Some prior reports of only minimally increased risk[11] were marred by the conversion of measured radiation dose to effective dose, a unit designed for assessing risk from whole-body radiation dose on the part of radiation workers or victims of environmental disasters. However, even methodologically sound prior reports, such as the RAD-IR study, found lower predicted risk than we report here (a median of 1.3–2.7 times baseline risk, depending on collimation), with their estimate of predicted risk, even for the large collimation condition, being 1.4 times baseline.[3] This discrepancy with our results is explained by the reliance on the part of prior investigators on the BEIR data for translation from radiation dose to tumor risk. However, the BEIR data reflect the condition of whole-body environmental exposure. In contrast, the projected risk we report here is based instead on the UK CT study[2]; in CT, patients undergo focal deposition of radiation to the target organ, as occurs as well during neurointerventions. The UK investigators reported a mean value of excess relative risk of 0.023/mGy, independent of age, in accord with a linear model of risk dependence on dose.

The BEIR investigators found increased risk of solid tumors of many types in various organs after whole-body exposure in atom bomb survivors. In focusing on the induction of brain tumors after head CT, the UK investigators found a positive (and independent) association between the scans and 2 categories of tumors: gliomas and meningiomas/schwannomas.[2] In terms of timeframe, the induction of solid tumors can span decades; the age range of patients included in the UK CT study was 6–45 years, and the maximal follow-up period was 23 years.

Several operator-dependent variables can dramatically reduce radiation dose, as seen by contrasting the wide-field uncollimated condition with the tightly collimated condition (ie, Tables 4 and 5). However, although, like the RAD-IR investigators, we do not have specific data on FOV size in our cohort, the ability to tightly collimate the FOV in neurointerventions is offset by the need to see critical surrounding vascular anatomy. Thus, most intracranial interventions probably approximate the wide-field condition. As mentioned, our system has been highly optimized to minimize radiation dose, with attention paid to technical factors, such as use of pulsed fluoroscopy, aggressive filtration, automated dose rate control, minimization of the air gap between patient and detector, maximal use of image-hold technologies (such as the overlay mode and care position for the Siemens system), and the use of age- and sex-specific lead shields, from the outset of this study.

One important limitation of our study is the relatively small sample size. In particular, the number of patients who underwent repeated neurointerventional procedures is small. Although we have projected risk values for this subset, they may not necessarily be representative of the population as a whole. Although our center is a high-volume tertiary pediatric cerebrovascular referral site, most conditions leading to neurointerventional procedures in children are rare, and a multi-institutional, national, or international data collection effort will be needed to materially increase the size of the cohort.

The predicted stochastic risk associated with neurointerventions in children undergoing multiple procedures we report here is sobering. Although most patients in our cohort underwent only 1 procedure, nearly one-third of the cohort underwent 2–3 procedures, and a smaller fraction underwent many more (Table 1). Although there may be some benefit to divided doses as compared with larger, single-procedure doses though mechanisms such as adaptive response,[12] this has yet to be explicitly demonstrated, and thus it may be assumed that the predicted risk across procedures is approximately additive.

CONCLUSIONS

All children undergoing neurointerventions face conditions that are life-threatening or that pose a risk of severe neurologic impairment, and thus the risk-benefit ratio impels treatment. However, in cases in which there are few data to buttress multiple repeated

interventions, such as staged embolization of highly complex brain AVMs with the goal of reducing flow rather than achieving definitive cure, the lifetime risks of radiation dose in children must be added to the procedural risks of vascular injury. Particularly in the youngest patients, it behooves the practitioner to weigh the risk of radiation dosage in comparing treatment alternatives and in determining the number of acceptable rounds of neurointerventional procedures. These data support the importance of developing alternative, nonfluoroscopic approaches for treating children, such as MR-based procedures.

Disclosures: Catherine Stamoulis—*UNRELATED: Consultancy:* Beth Israel Deaconess Medical Center, Comments: Entirely unrelated study on sleep.

REFERENCES

1. National Research Council (US) Committee to Assess Health Risks from Exposure to Low Levels of Ionizing Radiation. *Health Risks From Exposure to Low Levels of Ionizing Radiation: BEIR VII Phase 2.* Washington, DC: National Academies Press; 2006
2. Pearce MS, Salotti JA, Little MP, et al. **Radiation exposure from CT scans in childhood and subsequent risk of leukaemia and brain tumours: a retrospective cohort study.** *Lancet* 2012;380:499–505
3. Thierry-Chef I, Simon SL, Land CE, et al. **Radiation dose to the brain and subsequent risk of developing brain tumors in pediatric patients undergoing interventional neuroradiology procedures.** *Radiat Res* 2008;170:553–65
4. Thierry-Chef I, Simon SL, Miller DL. **Radiation dose and cancer risk among pediatric patients undergoing interventional neuroradiology procedures.** *Pediatr Radiol* 2006;36(Suppl 2):159–62
5. Petoussi-Henss N, Zankl M, Drexler G, et al. **Calculation of backscatter factors for diagnostic radiology using Monte Carlo methods.** *Phys Med Biol* 1998;43:2237–50
6. Wolfe TJ, Hussain SI, Lynch JR, et al. **Pediatric cerebral angiography: analysis of utilization and findings.** *Pediatr Neurol* 2009;40:98–101
7. Burger IM, Murphy KJ, Jordan LC, et al. **Safety of cerebral digital subtraction angiography in children: complication rate analysis in 241 consecutive diagnostic angiograms.** *Stroke* 2006;37:2535–39
8. Balter S, Schueler BA, Miller DL, et al. **Radiation doses in interventional radiology procedures: the RAD-IR study, part III: dosimetric performance of the interventional fluoroscopy units.** *J Vasc Interv Radiol* 2004;15:919–26
9. Miller DL, Balter S, Cole PE, et al. **Radiation doses in interventional radiology procedures: the RAD-IR study, part II: skin dose.** *J Vasc Interv Radiol* 2003;14:977–90
10. Miller DL, Balter S, Cole PE, et al. **Radiation doses in interventional radiology procedures: the RAD-IR study: part I: overall measures of dose.** *J Vasc Interv Radiol* 2003;14:711–27
11. Raelson CA, Kanal KM, Vavilala MS, et al. **Radiation dose and excess risk of cancer in children undergoing neuroangiography.** *AJR Am J Roentgenol* 2009;193:1621–28
12. Vares G, Wang B, Tanaka K, et al. **Mutagenic adaptive response to high-LET radiation in human lymphoblastoid cells exposed to X-rays.** *Mutat Res* 2011;706:46–52